

Supporting Information

A Novel AIE Chemosensor Based on Coumarin Functionalized Pillar[5]arene for Multi-analytes Detection and Application in Logic Gate

Hong-Qiang Dong ^a, Xiao-Qiang Ma ^a, Tai-Bao Wei ^{a*}, Qing-Yu Yang ^a, Yun-Fei Zhang ^a, Qin-Peng Zhang ^a, Hong Yao ^a, You-Ming Zhang ^{a, b} and Qi Lin ^{a*}

^a Key laboratory of Polymer Materials of Gansu Province, College of Chemistry and Chemical Engineering, Northwest Normal University, Lanzhou, Gansu, 730070, P. R. China.
E-mail: weitaibao@126.com, lingi2004@126.com

^b Deputy Director-General of Gansu Natural Energy Research Institute, Renmin Road 23, Lanzhou, Gansu, 730000, P. R. China.

Supporting Information:

Number of pages: 1-19

Number of Figure: S1-S31

Table of Contents

Synthesis and characterizations of compound PX	5
Fig. S1 ^1H NMR spectra of 1	6
Fig. S2 ^1H NMR spectra of PX	6
Fig. S3 ^{13}C NMR spectra of PX	7
Fig. S4 ESI-MS spectra of PX	7
Fig. S5 The chromaticity coordinates (CIE) of PX (1×10^{-4} M).....	8
Fig. S6 Fluorescence quantum yield according to the corresponding formula, using quinine sulfate as standard	9
Fig. S7 2D NOESY spectrum of PX (10mM) in DMSO- <i>d</i> 6 solution.....	9
Fig. S8 The XRD patterns of PX powder obtained from DMF (black) and DMF/H ₂ O (7:3, v/v) binary solution (red).....	9
Fig. S9 The frontier orbitals (HOMO and LUMO) of PX at the B3LYP/6-311G level.	
.....	10
Fig. S10 Color-filled RDG is surface plot: Non-covalent interaction (NCI) regions in EtP5 bound complexes.....	10
Fig. S11 Plot of the intensity at 400 nm for a mixture of PX (1.0×10^{-4} M) and Fe ³⁺ in DMF/H ₂ O binary solution (7:3, v/v) ($\lambda_{\text{ex}} = 385$ nm). Linear Equation: $Y = -131.58X + 517.399$, $R^2 = 0.9935$, LOD = 1.67×10^{-7} M	11
Fig. S12 Plot of the intensity at 400 nm for a mixture of PX (1.0×10^{-4} M) and Ba ²⁺ in DMF/H ₂ O binary solution (7:3, v/v) ($\lambda_{\text{ex}} = 385$ nm). Linear Equation: $Y = -374.03X + 673.908$, $R^2 = 0.9947$, LOD = 5.89×10^{-8} M	11
Fig. S13 Fluorescence emission ($\lambda_{\text{ex}} = 385$ nm) spectra of PX-Fe³⁺ (1.0×10^{-4} M) with different anions (F ⁻ , Cl ⁻ , Br ⁻ , I ⁻ , AcO ⁻ , HSO ₄ ⁻ , H ₂ PO ₄ ⁻ , ClO ₄ ⁻ , CN ⁻ , SCN ⁻ , N ₃ ⁻ , OH ⁻ and S ²⁻) in the DMF/H ₂ O (7:3, v/v) binary solution in response (3.0 equiv.).....	12
Fig. S14 Fluorescence emission ($\lambda_{\text{ex}} = 385$ nm) spectra of PX-Ba²⁺ (1.0×10^{-4} M) with different anions (F ⁻ , Cl ⁻ , Br ⁻ , I ⁻ , AcO ⁻ , HSO ₄ ⁻ , H ₂ PO ₄ ⁻ , ClO ₄ ⁻ , CN ⁻ , SCN ⁻ , N ₃ ⁻ , OH ⁻ and S ²⁻) in the DMF/H ₂ O (7:3, v/v) binary solution in response (3.0 equiv.).....	12

Fig. S15 Plot of the intensity at 385 nm for a mixture of PX- Fe³⁺ (1.0×10^{-4} M; 5.67 equiv) and H ₂ PO ₄ ⁻ in DMF/H ₂ O (7:3, v/v) binary solution. Linear Equation: Y = 163.804X + 135.447, R ² = 0.9952, LOD = 1.50×10^{-7} M.....	13
Fig. S16 Plot of the intensity at 385 nm for a mixture of PX- Ba²⁺ (1.0×10^{-4} M; 5.33 equiv) and CN ⁻ in DMF/H ₂ O (7:3, v/v) binary solution. Linear Equation: Y = 42.00X + 363.969, R ² = 0.9983, LOD = 6.20×10^{-7} M.....	13
Fig. S17 Fluorescence response of PX-Fe³⁺ (1.0×10^{-4} M) in the presence of H ₂ PO ₄ ⁻ (5.0 equiv.) and 5.0 equiv.other anions (F ⁻ , Cl ⁻ , Br ⁻ , I ⁻ , OH ⁻ ,HSO ₄ ⁻ ,S ²⁻ , SCN ⁻ , AcO ⁻ , ClO ₄ ⁻ , CN ⁻ ,and N ₃ ⁻) in DMF/H ₂ O (7:3, v/v) binary solution. (λ_{ex} = 385 nm).....	14
Fig. S18 Fluorescence response of PX-Ba²⁺ (1.0×10^{-4} M) in the presence of CN ⁻ ions (5.0 equiv.) and 5.0 equiv.other anions (F ⁻ , Cl ⁻ , Br ⁻ , I ⁻ , OH ⁻ ,HSO ₄ ⁻ ,S ²⁻ , SCN ⁻ , AcO ⁻ , ClO ₄ ⁻ , CN ⁻ ,and N ₃ ⁻) in DMF/H ₂ O (7:3, v/v) binary solution. (λ_{ex} = 385 nm).....	14
Fig. S19 Partial ¹ H NMR spectra of PX in DMSO- <i>d</i> ₆ with different equivalents of Ba ²⁺ (a). 0 equiv. (b). 0.8 equiv. (c). 1.6equiv. (d). 2.4 equiv. (e). 3.2 equiv.	14
Fig. S20 SEM images of (a) PX + Fe ³⁺ ; (b) PX + Fe ³⁺ + H ₂ PO ₄ ⁻	15
Fig. S21 FT-IR spectra of powdered PX (black), PX+Fe³⁺ (red), and PX+Fe³⁺ + H ₂ PO ₄ ⁻ (blue).....	15
Fig. S22 FT-IR spectra of powdered PX (black), PX+Ba²⁺ (green), and PX+ Ba²⁺ + CN ⁻ (red).....	15
Fig. S23 powder XRD patterns of the PX-Fe³⁺ (black), PX-Fe³⁺+H₂PO₄ (red), PX+Ba²⁺ (blue)and PX+Ba²⁺+CN ⁻ (purple).....	15
Fig. S24 The Job's plot examined between Fe ³⁺ and PX , indicating the 1:1 stoichiometry, which was carried out by fluorescence spectra.	16
Fig. S25 The Job's plot examined between Ba ²⁺ and PX , indicating the 1:1 stoichiometry, which was carried out by fluorescence spectra.	16
Fig. S26 ESI-MS spectra of [PX +Fe+3(CHCl ₃)] ³⁺	17
Fig. S27 ESI-MS spectra of (PX +Ba) ²⁺	17
Fig. S28 Synthesis and characterizations of compound 2	18
Fig. S29 ¹ H NMR spectra of 2	19

Fig. S30 Fluorescence emission ($\lambda_{\text{ex}} = 320$ nm) spectra of 2 (1.0×10^{-4} M) with metal ions [Zn ²⁺ , Pb ²⁺ , Cd ²⁺ , Fe ³⁺ , Co ²⁺ , Hg ²⁺ , Ag ⁺ , Ca ²⁺ , Mg ²⁺ , Ba ²⁺ , Cr ³⁺ , Eu ³⁺ , La ³⁺ and Al ³⁺ (2.0 equiv.)] in the DMF/H ₂ O (7:3, v/v) binary solution (2.0 equiv.).....	19
Fig. S31 Fluorescence color change (under the UV lamp, at $\lambda_{\text{ex}} = 385$ nm) of silica gel plate treated by PX after addition different concentration Fe ³⁺ , Ba ²⁺ , H ₂ PO ₄ ⁻ and CN ⁻	20

1. Synthesis and characterizations of compound **PX**

Synthesis of pillar[5]arene (**1**): 1-(6-dibromohexane)-4-methoxybenzene (2.87 g, 10 mmol) and 1, 4-dimethoxybenzene (8.64 g, 80 mmol) in 1, 2-dichloroethane (250 mL), paraformaldehyde (2.5 g, 80 mmol) was added. Then, boron trifluoride diethyl etherate ($\text{BF}_3 \cdot \text{O}(\text{C}_2\text{H}_5)_2$, 8 mL) was added to the solution and the mixture was stirred at 30°C for 30 min. The solution was poured into water (150 mL) to quench the reaction. As shown in Scheme S1. The mixture was extracted and the aqueous layer was removed. The organic layer was dried over anhydrous Na_2SO_4 and evaporated to afford the crude product, which was isolated by column chromatography using petroleum ether/Dichloromethane/ethyl acetate (100:25:1, v/v/v) to give Compound **1** as a white solid (1.06 g, 37%).

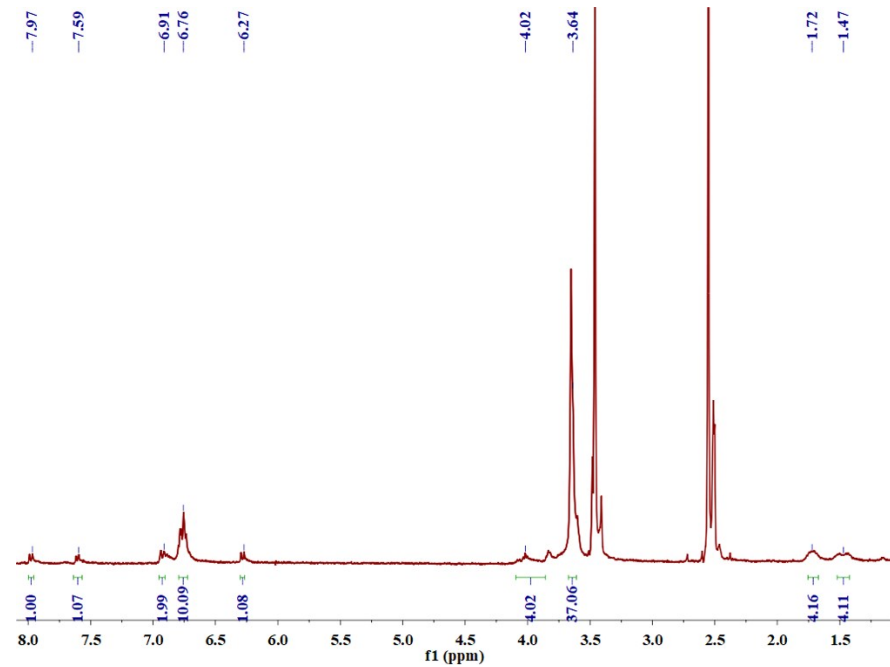
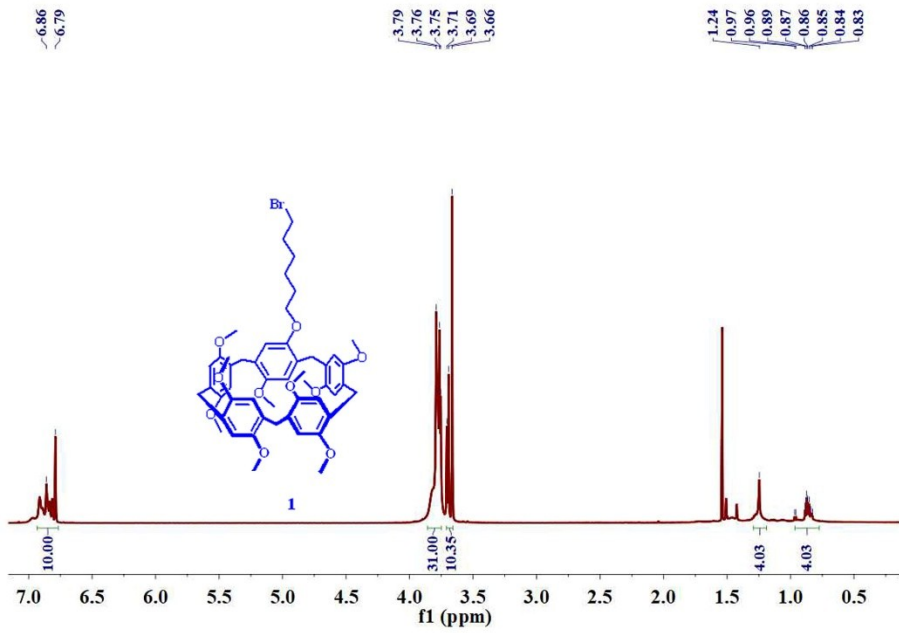
Synthesis of **PX**: Pillar[5]arene(**1**) (0.9 g, 1 mmol) and 7-hydroxycoumarin (0.2 g, 1.2 mmol) were added to a solution of KI (0.498 g, 3 mmol) and K_2CO_3 (0.828 g, 6 mmol) in N,N-Dimethylformamide/acetone (3:50, v/v). The mixture was heated under nitrogen atmosphere and refluxed for 3 day. As shown in Scheme 1. After the reaction is completed, it is washed with sodium hydroxide solution to remove excess 7-hydroxycoumarin. The crude product was isolated by column chromatography using petroleum ether/ethyl acetate (20:1, v/v) to get a white solid **PX** (0.72 g, 80%). M.P.: 113-115 °C. ^1H NMR (600 MHz, CDCl_3 , room temperature) δ (ppm): 7.97(d, $J=14.4$ Hz 1H), 7.59(d, $J=10.2$ Hz, 1H), 6.91(d, $J=15$ Hz, 2H), 6.76(m, 10H), 6.27(d, $J=14.4$ Hz, 1H), 4.02(t, $J=9.6$ Hz, 4H), 3.64(s, 37H), 1.72(m, 4H), 1.47(m, 4H). ^{13}C NMR (150 MHz, CDCl_3 , room temperature) δ (ppm): 160.8, 159.0, 156.5, 147.4, 143.5, 129.4, 113.8, 111.1, 104.1, 68.7, 56.1, 30.1, 25.9. ESI-MS m/z : $[\text{PX}+\text{H}]^+$ Calcd $\text{C}_{59}\text{H}_{64}\text{O}_{13}$ 980.44, found 981.44

Calculation formula of LOD

Linear Equation: $Y = aX + b$

$$\delta = \sqrt{\frac{\sum_{i=1}^N (F_i - \bar{F})^2}{N-1}} \quad (N = 20)$$

$$\text{LOD} = K \times \delta/S \quad (K = 3, S = a \times 10^6)$$



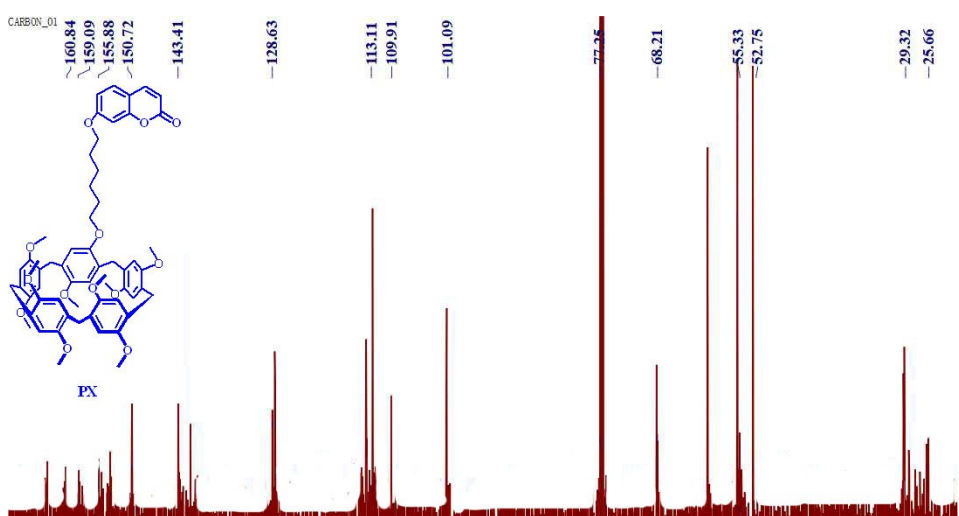


Fig. S3 ^{13}C NMR spectra of PX in CDCl_3

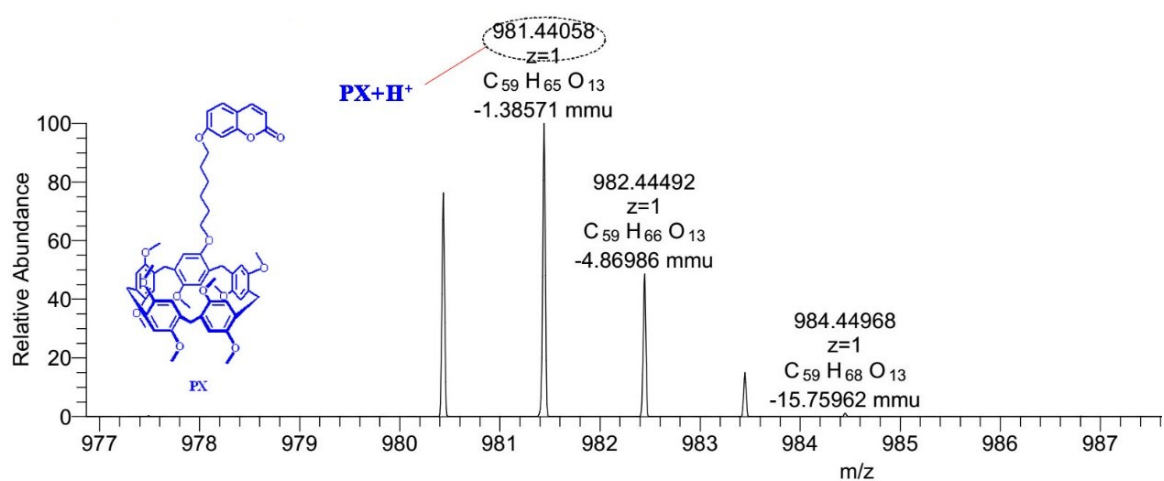


Fig. S4 ESI-MS spectra of PX.

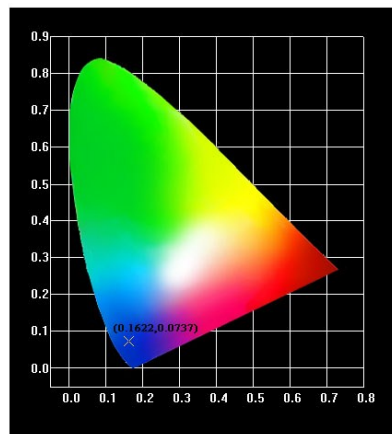


Fig. S5 The Commission Internationale de L'Eclairage (CIE) for **PX** (1.0×10^{-4} M) in DMF/H₂O (7:3v/v) binary solution

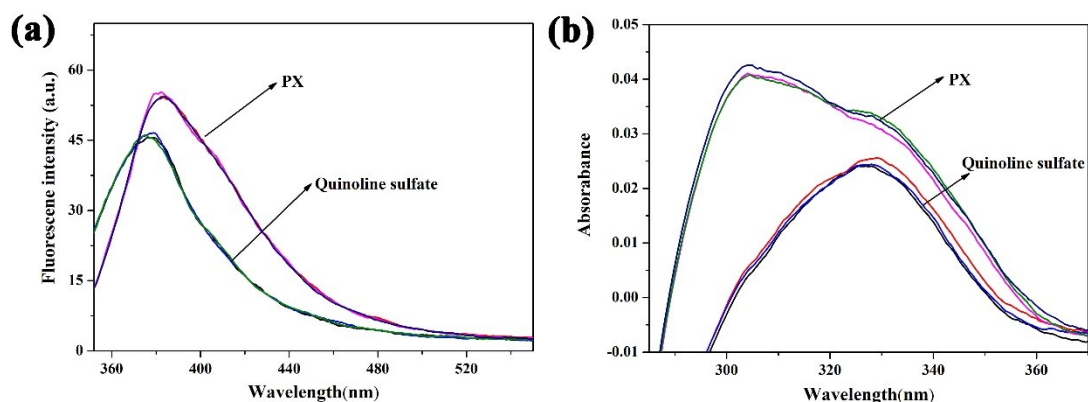


Fig. S6 Fluorescence quantum yield according to the corresponding formula, using quinoline sulfate as standard

The fluorescence quantum yield of the sample was calculated using quinine sulfate as the standard ($\Phi_{\text{std}} = 0.55$). In this equation, Φ_{unk} and Φ_{std} are the fluorescence quantum yields of the sample and the standard, respectively; I_{unk} and I_{std} are the integral areas of the fluorescent spectra, respectively; A_{unk} and A_{std} are the absorbances of the sample and the standard at the excitation wavelength, respectively.

$$\Phi_{\text{unk}} = \Phi_{\text{std}} \times (I_{\text{unk}} / I_{\text{std}}) \times (A_{\text{std}} / A_{\text{unk}}) \quad \Phi_{\text{std}} = 0.55$$

$$I_{\text{unk}}: 7.2993 \quad I_{\text{std}}: 7.2956 \quad A_{\text{std}}: 0.028 \quad A_{\text{unk}}: 0.044$$

$$\Phi_{\text{unk}} = 0.55 \times (7.2993 / 7.2956) \times (0.028 / 0.044) = 0.350$$

Fluorescence quantum yield: 35.0%

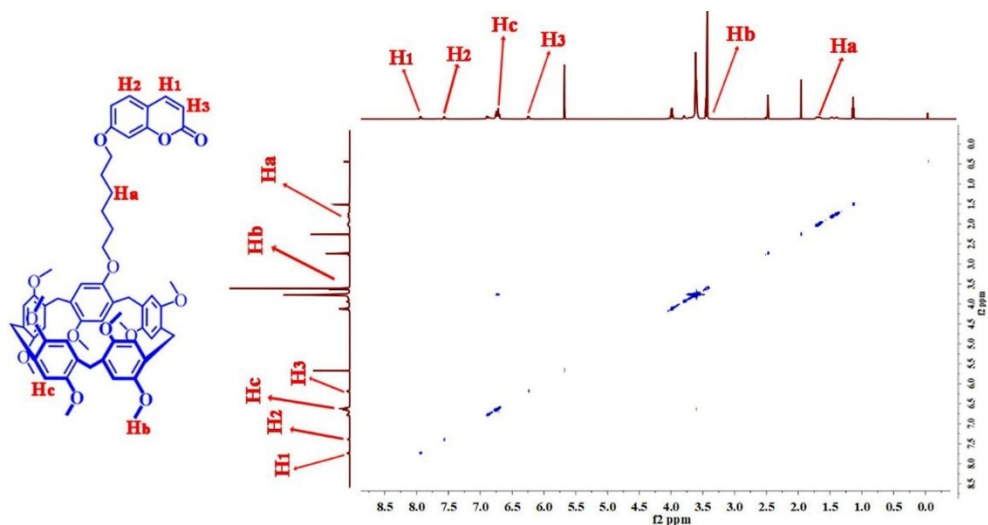


Fig. S7 2D NOESY spectrum of **PX** (10mM) in DMSO-*d*6 solution

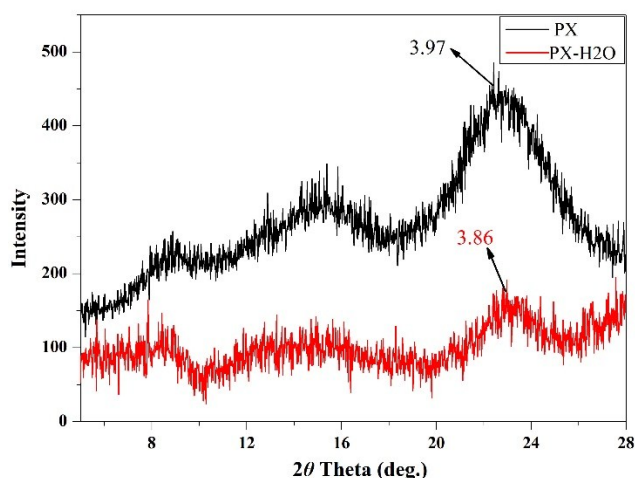


Fig. S8 The XRD patterns of **PX** powder obtained from DMF (black) and DMF/H₂O (7:3, v/v) binary solution (red)

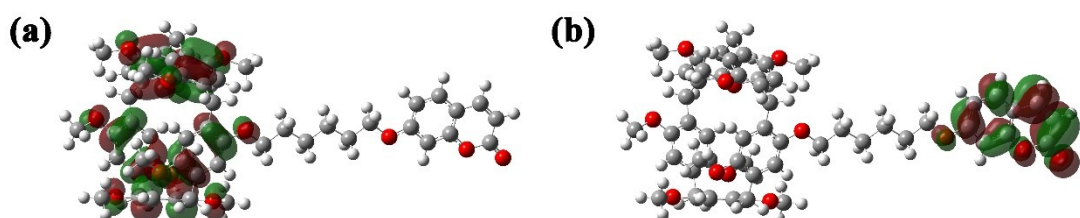


Fig. S9 The frontier orbitals (HOMO and LUMO) of **PX** at the B3LYP/6-311G level

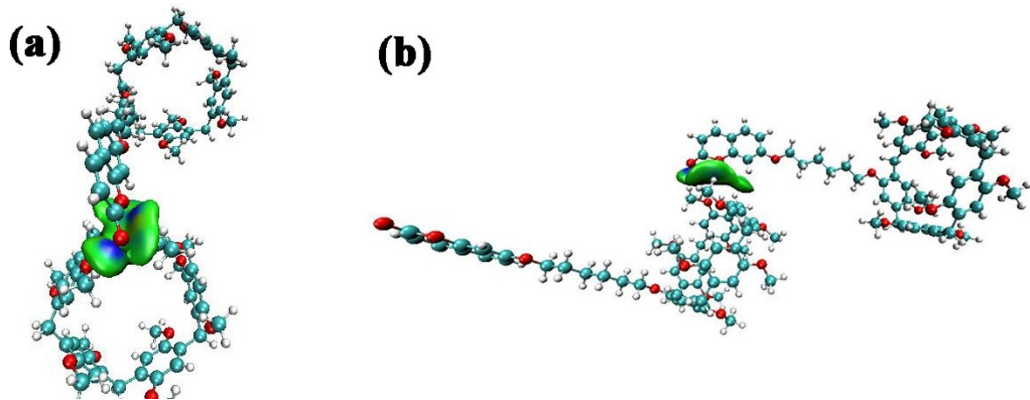


Fig. S10 Color-filled RDG isosurface plot: Non-covalent interaction (NCI) regions in EtP5 bound complexes

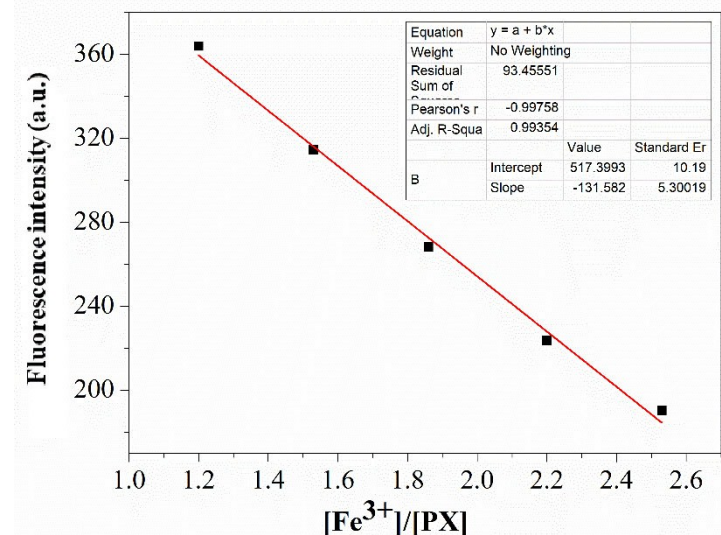


Fig. S11 Photograph of the linear range for Fe^{3+}

The result of the analysis as follows:

$$\text{Linear Equation: } Y = -131.58X + 517.399, \quad R^2 = 0.9935,$$

$$S = 131.58 \times 10^6$$

$$\text{LOD} = K \times \delta/S = 1.67 \times 10^{-7} \text{ M} \quad (K = 3)$$

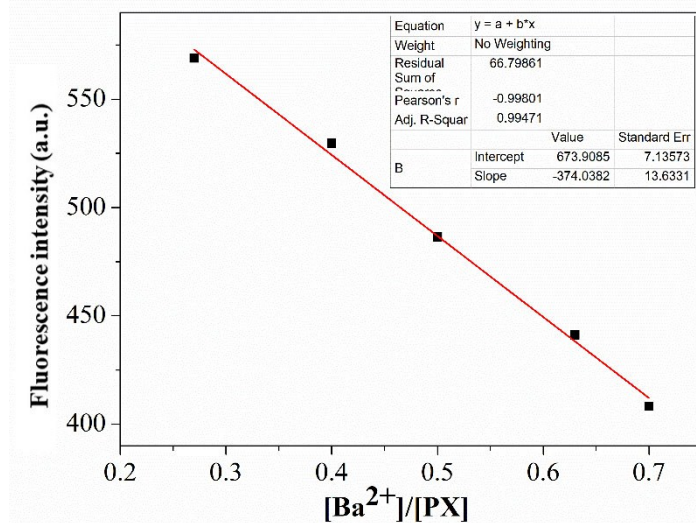


Fig. S12 Photograph of the linear range for Ba^{2+}

The result of the analysis as follows:

Linear Equation: $Y = -374.03X + 673.908$, $R^2 = 0.9947$,

$S = 374.03 \times 10^6$

$\text{LOD} = K \times \delta/S = 5.89 \times 10^{-8} \text{ M}$ ($K = 3$)

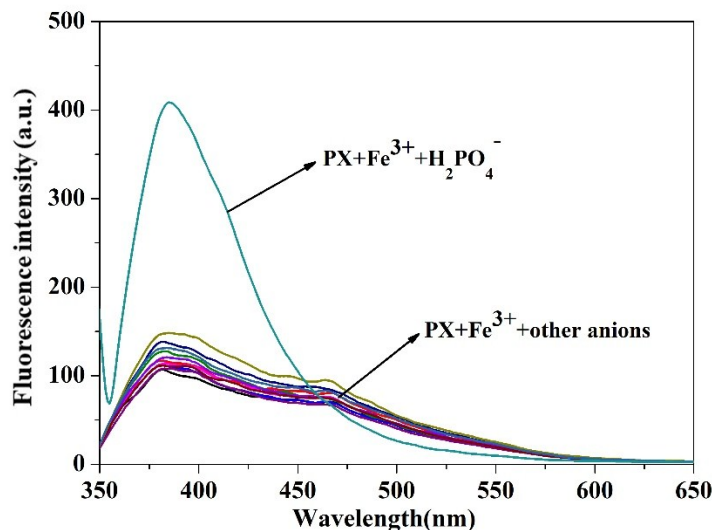


Fig. S13 Fluorescence emission ($\lambda_{\text{ex}} = 320\text{nm}$) spectra of PX-Fe^{3+} ($1.0 \times 10^{-4} \text{ M}$) with different anions (F^- , Cl^- , Br^- , I^- , AcO^- , HSO_4^- , H_2PO_4^- , ClO_4^- , CN^- , SCN^- , N_3^- , OH^- and S^{2-}) in the $\text{DMF}/\text{H}_2\text{O}$ (7:3, v/v) binary solution in response (3.0 equiv.).

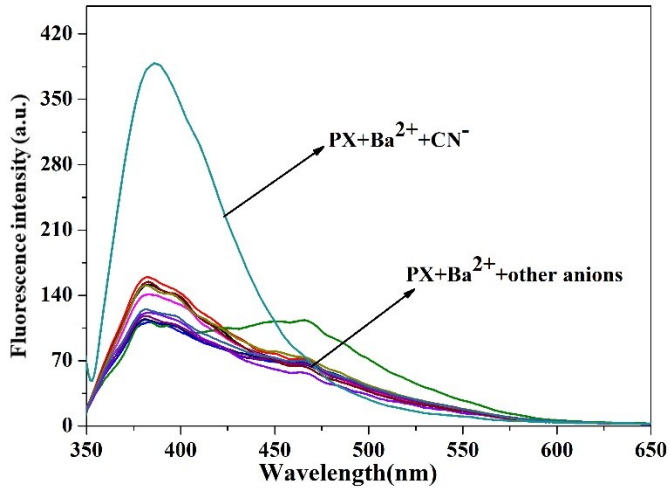


Fig. S14 Fluorescence emission ($\lambda_{\text{ex}} = 320\text{nm}$) spectra of **PX-Ba²⁺** ($1.0 \times 10^{-4} \text{ M}$) with different anions (F⁻, Cl⁻, Br⁻, I⁻, AcO⁻, HSO₄⁻, H₂PO₄⁻, ClO₄⁻, CN⁻, SCN⁻, N₃⁻, OH⁻ and S²⁻) in the DMF/H₂O (7:3, v/v) binary solution in response (3.0 equiv.).

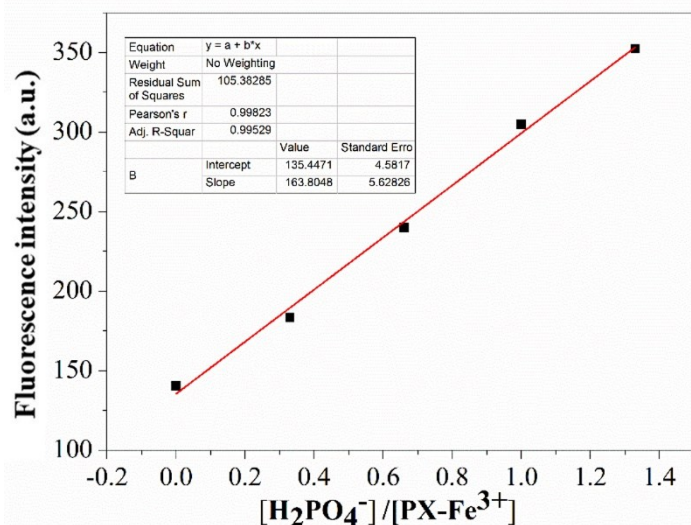


Fig. S15 Photograph of the linear range for H₂PO₄⁻
The result of the analysis as follows:

Linear Equation: $Y = 163.80X + 135.447$, $R^2 = 0.9952$,

$S = 16.80 \times 10^6$

$\text{LOD} = K \times \delta/S = 1.50 \times 10^{-7} \text{ M}$ ($K = 3$)

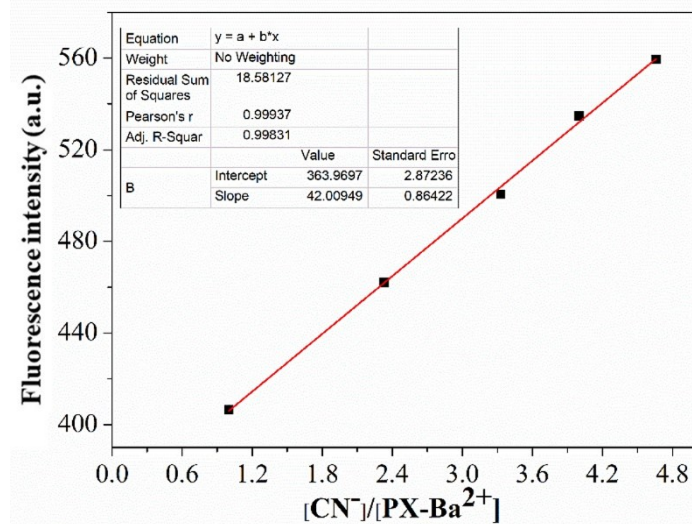


Fig. S16 Photograph of the linear range for CN⁻

The result of the analysis as follows:

Linear Equation: Y = 42.00X + 363.969, R² = 0.9983,

S = 42.00 × 10⁶

LOD = K × δ/S = 6.20 × 10⁻⁷ M (K = 3)

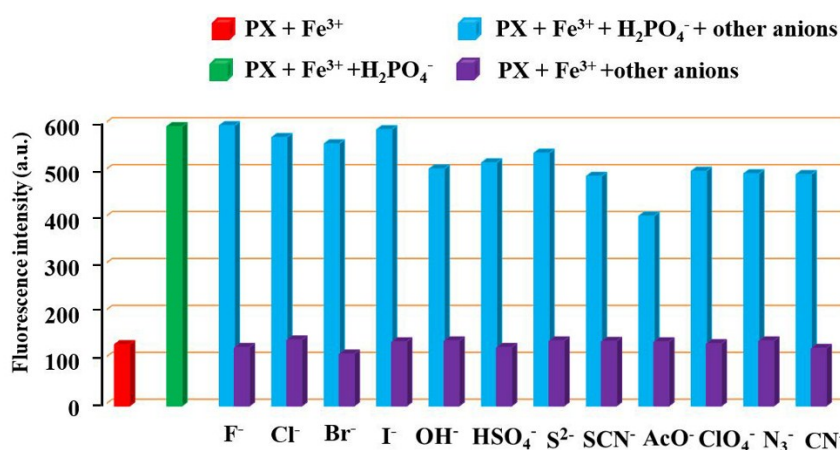


Fig. S17 Fluorescence response of PX-Fe³⁺(1.0×10⁻⁴ M) in the presence of H₂PO₄⁻ions (5.0 equiv.) and 5.0 equiv. other anions (F⁻, Cl⁻, Br⁻, I⁻, OH⁻, HSO₄⁻, S²⁻, SCN⁻, AcO⁻, ClO₄⁻, N₃⁻ and CN⁻) in DMF/H₂O (7:3, v/v) binary solution.

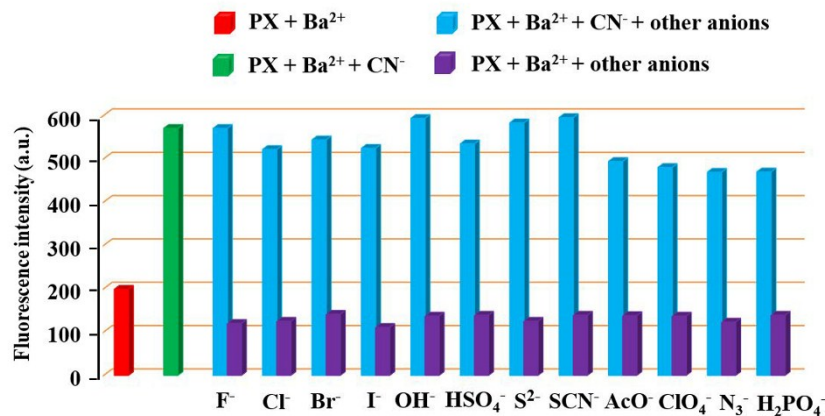


Fig. S18 Fluorescence response of **PX**-Ba²⁺(1.0×10⁻⁴ M) in the presence of CN⁻ ions (5.0 equiv.) and 5.0 equiv. other anions (F⁻, Cl⁻, Br⁻, I⁻, OH⁻, HSO₄⁻, S²⁻, SCN⁻, AcO⁻, ClO₄⁻, N₃⁻ and H₂PO₄⁻) in DMF/H₂O (7:3, v/v) binary solution.

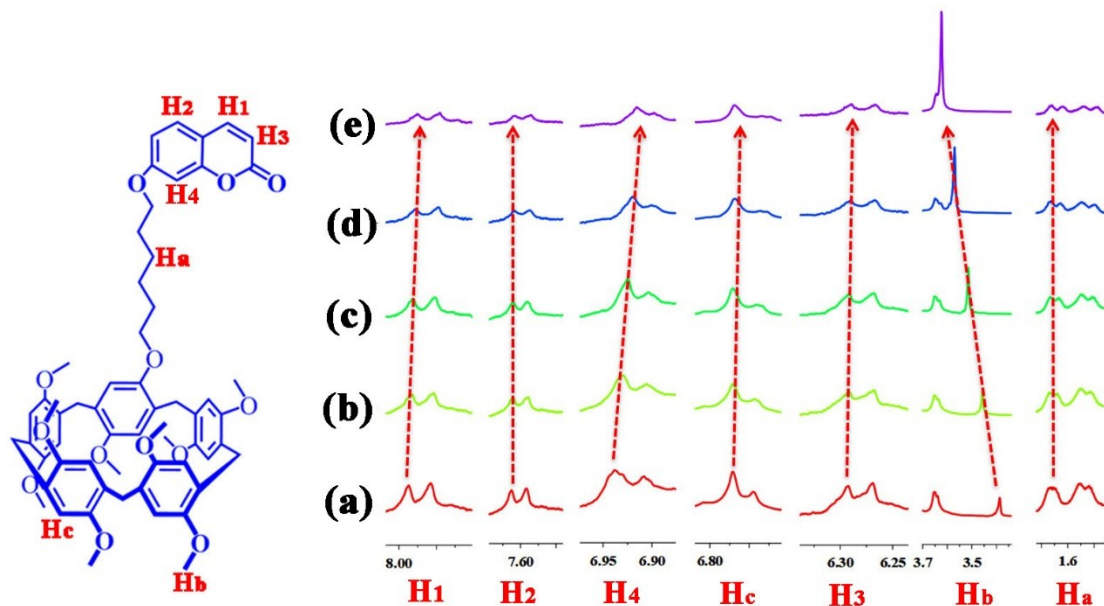


Fig. S19 Partial ¹H NMR spectra of **PX** in DMSO-d6 with different equivalents of Ba²⁺(a). 0 equiv. (b). 0.8 equiv. (c). 1.6equiv. (d). 2.4 equiv. (e). 3.2 equiv.

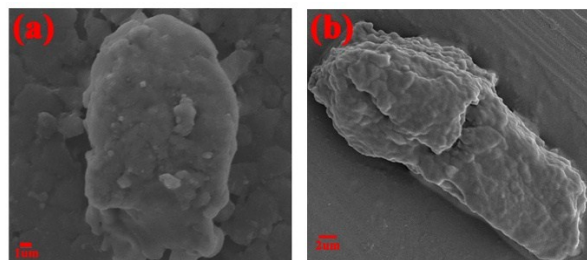


Fig. 20 SEM images of (a) **PX** + Fe³⁺; (b) **PX** + Fe³⁺ + H₂PO₄⁻

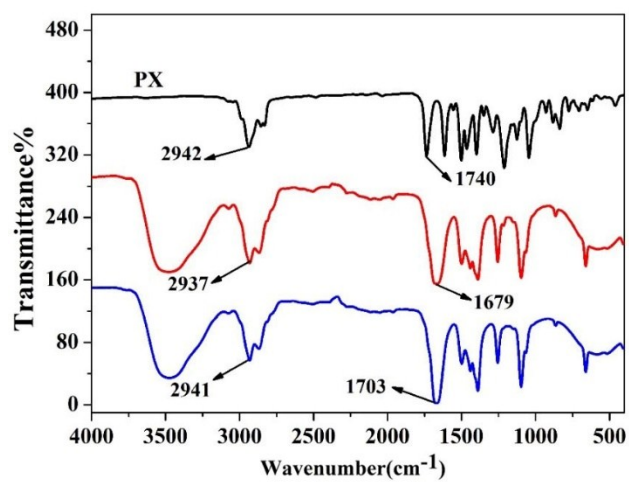


Fig. S21 FT-IR spectra of powdered **PX** (black), **PX+Fe³⁺** (red), and **PX+Fe³⁺ + H₂PO₄⁻** (blue).

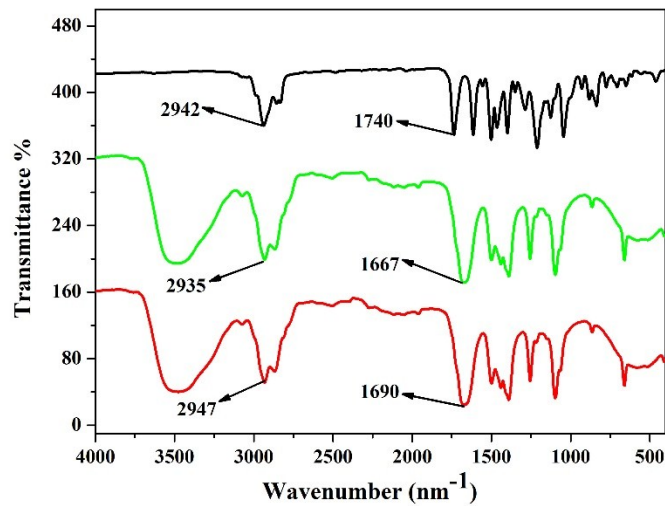


Fig. S22 FT-IR spectra of powdered **PX** (black), **PX + Ba²⁺** (green), and **PX + Ba²⁺ + CN⁻** (red)

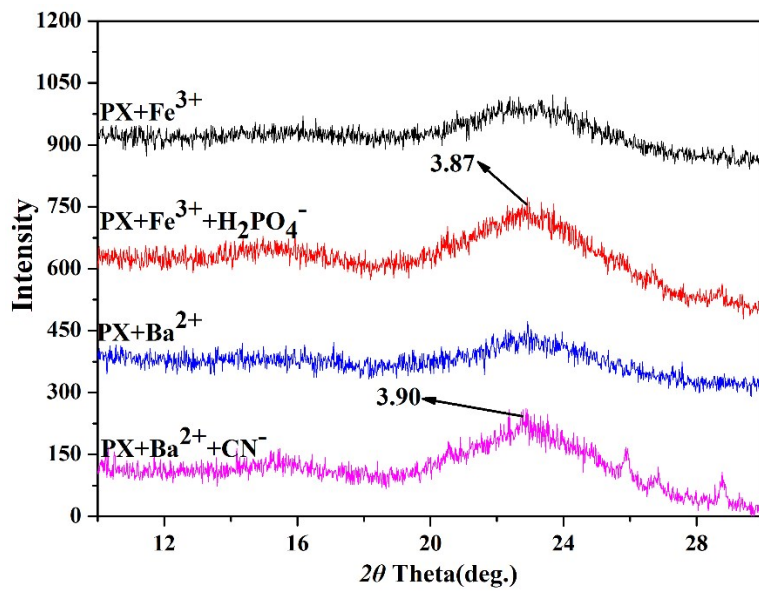


Fig. S23 The powder XRD patterns of the $\text{PX}-\text{Fe}^{3+}$ (black), $\text{PX}-\text{Fe}^{3+}+\text{H}_2\text{PO}_4^-$ (red), $\text{PX}+\text{Ba}^{2+}$ (blue) and $\text{PX}+\text{Ba}^{2+}+\text{CN}^-$ (purple)

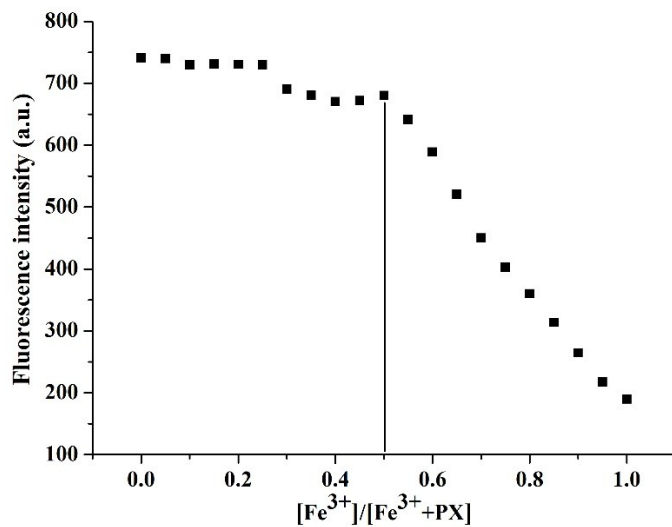


Fig. S24 The Job's plot examination between **PX** and Fe^{3+} , indicating the 1:1 stoichiometry.

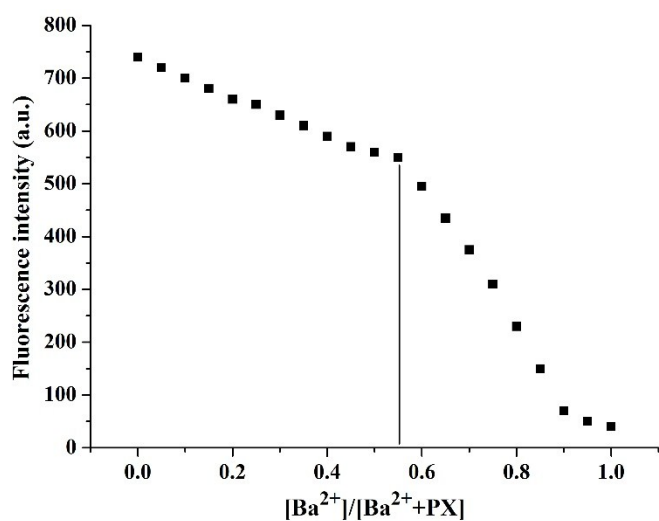


Fig. S25 The Job's plot examination between PX and Ba^{2+} , indicating the 1:1 stoichiometry.

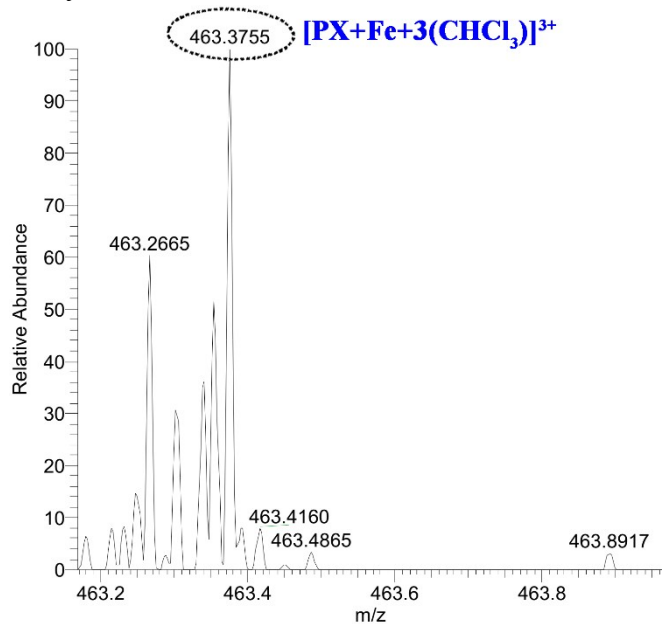


Fig. S26 ESI-MS of an equimolar solution of $[\text{PX}+\text{Fe}+3(\text{CHCl}_3)]^{3+}$ exhibited a peak at $m/z = 463.37$, corresponding to $[\text{PX}+\text{Fe}+3(\text{CHCl}_3)]^{3+}$ which revealed a 1:1 stoichiometry for the complexation between PX and Fe^{3+}

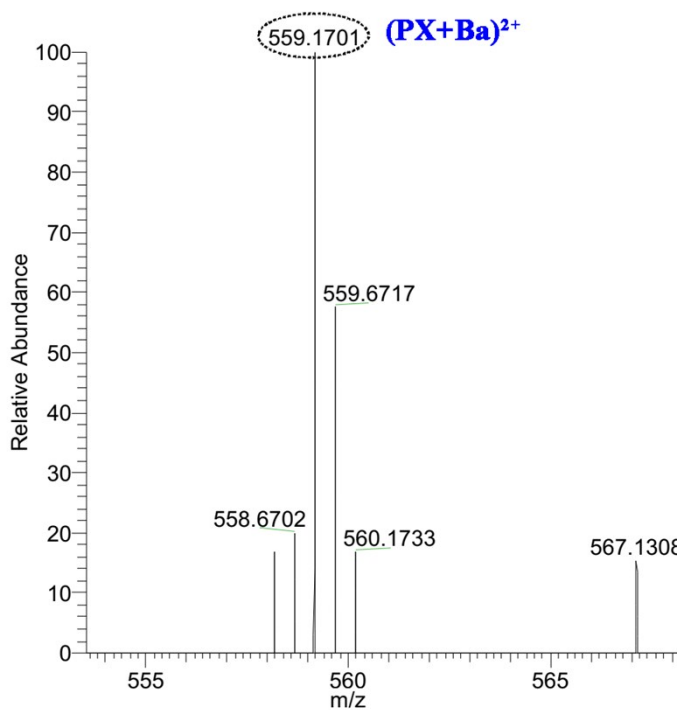


Fig. S27 ESI-MS of an equimolar solution of $(\text{PX} + \text{Ba})^{2+}$ exhibited a peak at $m/z = 559.17$, corresponding to $(\text{PX} + \text{Ba})^{2+}$ which revealed a 1:1 stoichiometry for the complexation between **PX** and Ba^{2+}

1-(6-dibromohexane)-4-methoxybenzene (0.5 g, 2 mmol) and 7-hydroxycoumarin (0.2 g, 1.5 mmol) were added to a solution of KI (0.498 g, 3 mmol) and K_2CO_3 (0.828 g, 6 mmol) in acetone 50 ml. The mixture was heated under nitrogen atmosphere and refluxed for 3 day. As shown in Scheme 2. The crude product was isolated by column chromatography using petroleum ether/ethyl acetate (15:1, v/v) to get a white solid **2** (0.22 g, 37%)

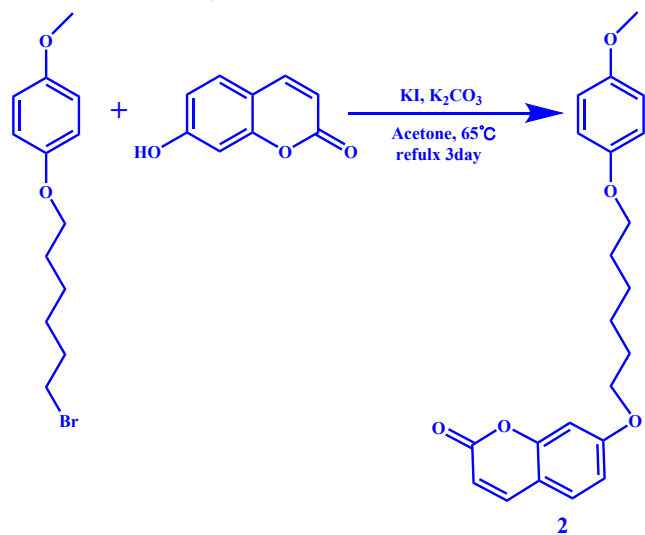


Fig. S28 Scheme 2. Synthetic route to compound **2**

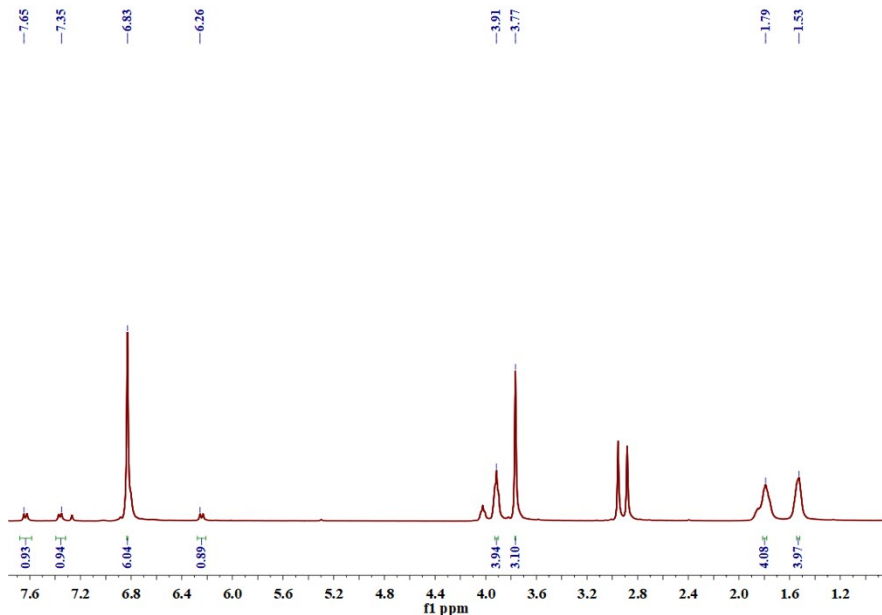


Fig. S29 ^1H NMR spectra of **2** in CDCl_3

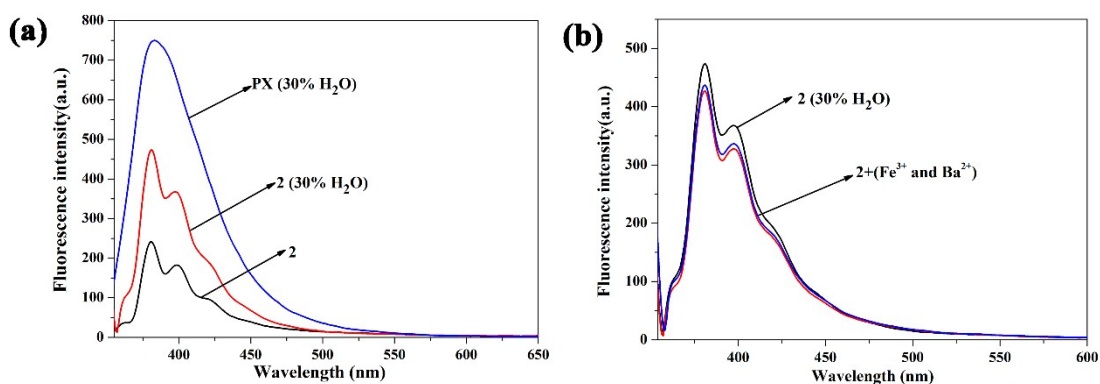


Fig. S30 (a) Fluorescence emission ($\lambda_{\text{ex}} = 320 \text{ nm}$) spectra of **2**, **PX** and **2** in DMF/H₂O binary solution with 30% water fraction, solution concentration: $1.0 \times 10^{-4} \text{ M}$ (b) Fluorescence emission ($\lambda_{\text{ex}} = 320 \text{ nm}$) spectra of **2** ($1.0 \times 10^{-4} \text{ M}$) with metal ions [Fe^{3+} , Ba^{2+} (2.0 equiv.)] in the DMF/H₂O (7:3, v/v) binary solution.

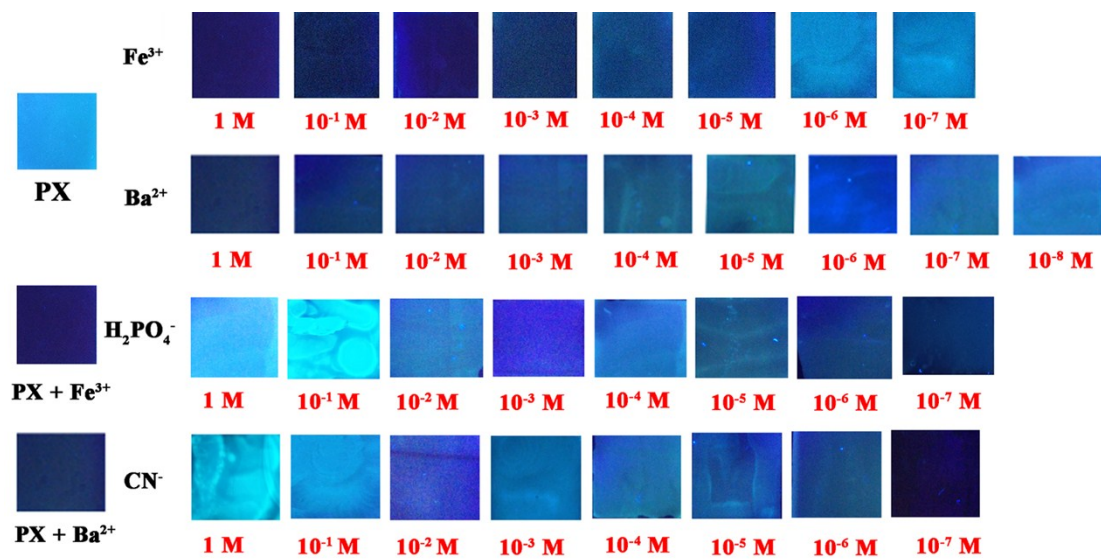


Fig. S31 Fluorescence color change (under the UV lamp, at $\lambda_{\text{ex}} = 365 \text{ nm}$) of silica gel plate treated by **PX** after addition different concentration Fe^{3+} (from 1.0 M to $1 \times 10^{-7} \text{ M}$), Ba^{2+} (from 1.0 M to $1 \times 10^{-8} \text{ M}$), H_2PO_4^- (from 1.0 M to $1 \times 10^{-7} \text{ M}$) and CN^- (from 1.0 M to $1 \times 10^{-7} \text{ M}$).